THE ASTROPHYSICAL JOURNAL, 540:L9–L12, 2000 September 1

DYNAMICAL MASS ESTIMATES FOR THE HALO OF M31 FROM KECK SPECTROSCOPY[1]

N. WYN EVANS,[2] MARK I. WILKINSON,[3] PURAGRA GUHATHAKURTA,[4,5] EVA K. GREBEL,[6,7] AND STEVEN S. VOGT[4]

Received 2000 May 1; accepted 2000 July 7; published 2000 August 18

ABSTRACT

The last few months have seen the measurements of the radial velocities of all of the dwarf spheroidal companions to the Andromeda galaxy (M31) using the spectrographs (HIRES and LRIS) on the Keck Telescope. This Letter summarizes the data on the radial velocities and distances for all the companion galaxies and presents new dynamical modeling to estimate the mass of the extended halo of M31. The best-fit values for the total mass of M31 are $\sim(7\text{–}10) \times 10^{11}\ M_\odot$, depending on the details of the modeling. The mass estimate is accompanied by considerable uncertainty caused by the small size of the data set; for example, the upper bound on the total mass is $\sim 24 \times 10^{11}\ M_\odot$, while the lower bound is $\sim 3 \times 10^{11}\ M_\odot$. These values are less than the most recent estimates of the most likely mass of the Milky Way halo. Bearing in mind all the uncertainties, a fair conclusion is that the M31 halo is roughly as massive as that of the Milky Way halo. There is no dynamical evidence for the widely held belief that M31 is more massive—it may even be less massive.

Subject headings: galaxies: halos — galaxies: individual (M31) — galaxies: kinematics and dynamics — galaxies: structure — Local Group

1. INTRODUCTION

Dynamical studies of the two largest members of the Local Group—the Milky Way and the Andromeda (M31) galaxies—are of particular interest. The mass of M31 is well constrained on a scale of a few tens of kiloparsecs from the optical and H I rotation curves (Braun 1991) and from the kinematics of the planetary nebulae and globular cluster populations (e.g., Evans & Wilkinson 2000). To probe much larger radii and estimate the total mass of the M31 halo, it is to the satellite galaxy population that we must turn. Here, there have been dramatic developments in the last few years. The advent of wide-field imaging surveys (Armandroff, Davies, & Jacoby 1998; Karachentsev & Karachentseva 1999; Armandroff, Jacoby, & Davies 1999) has led to the discovery of three new dwarf spheroidal galaxies (dSphs): And V, And VI (Peg dSph), and Cas dSph. In all, the entourage of galaxies accompanying M31 now numbers as many as 15, although the status of two of these (Pegasus and IC 1613) is perhaps unclear since opinions differ as to whether they are close enough to be bound (Mateo 1998; Grebel 1999; Courteau & van den Bergh 1999).

For the Milky Way, the data set of the 11 companion galaxies, as well as the distant globular clusters, has often been exploited to estimate the total mass of the Milky Way halo. The older techniques of virial estimators have nowadays been superseded by more sophisticated Bayesian likelihood estimators (Little & Tremaine 1987). The most recent analysis by Wilkinson & Evans (1999) found a total mass for the Milky Way halo of $\sim 19^{+36}_{-17} \times 10^{11}\ M_\odot$, with the large error bars reflecting the small sample size and the uncertainties in the proper motions. Hitherto, the satellites of M31 have received scant attention. Evans & Wilkinson (2000) looked at all the available published data on 10 of the satellite galaxies and found a rather low mass of $\sim 12.3^{+18}_{-6} \times 10^{11}\ M_\odot$. This raises the possibility that the Milky Way Galaxy may be the largest member of the Local Group.

Here, we exploit recent stellar velocity measurements with the spectrographs on the Keck Telescopes. The new observations are reported in detail by Guhathakurta et al. (2000a) and Guhathakurta, Reitzel, & Grebel (2000b). The results enhance the data set on the radial velocities of the companion galaxies of M31 by 50% and are used to provide the most reliable estimate of the mass of the extended halo of M31 to date.

2. DATA

2.1. *Radial Velocity Measurements*

The radial velocities of eight of the companions to M31 have been known for some time based on one or more of the following techniques: H I 21 cm measurements, optical absorption line spectra of the integrated light of galaxy cores/nuclei, bulges, or globular clusters, or optical emission line spectra of H II regions. The data are recorded in the upper panel of Table 1. These techniques are not easily applicable to galaxies of low surface brightness and/or low gas content. Consequently, until very recently, the radial velocities of the six dSph companions (And I, And II, And III, And V, And VI, and Cas dSph) remained unmeasured. They require 8–10 m–class telescopes and efficient spectrographs for spectroscopy of individual red giant stars. Côté et al. (1999) have recently provided the first kinematic study of And II. They used the High-Resolution Echelle Spectrometer (HIRES; Vogt et al. 1994) on the 10 m Keck I Telescope to measure the radial velocities of a few red giants in each dwarf galaxy. Guhathakurta et al. (2000a, 2000b) provide the data on the outstanding five dSphs. Using the Low-Resolution Imaging Spectrometer (LRIS; Oke et al. 1995) on the Keck II Telescope, they obtained velocity measurements for nearly a hundred red giants in And I, And III, And V, and And VI. Guhathakurta et al. (2000a, 2000b)

[1] Based in part on data collected at W. M. Keck Observatory, which is operated as a scientific partnership among the California Institute of Technology, the University of California, and the National Aeronautics and Space Administration. The Observatory was made possible by the generous financial support of the W. M. Keck Foundation.

[2] Theoretical Physics, 1 Keble Road, Oxford, OX1 3NP, England, UK; nwe@thphys.ox.ac.uk.

[3] Institute of Astronomy, Madingley Road, Cambridge, CB3 OHA, England, UK; markw@ast.cam.ac.uk.

[4] UCO/Lick Observatory, Department of Astronomy and Astrophysics, University of California, Santa Cruz, CA 95064; raja@ucolick.org, vogt@ucolick.org.

[5] Alfred P. Sloan Research Fellow.

[6] University of Washington, Department of Astronomy, Box 35158, Seattle, WA 98195-1580; and Max Planck Institute for Astronomy, Heidelberg, Germany; grebel@mpia-hd.mpg.de.

[7] Hubble Fellow.

TABLE 1
DATA ON M31 AND ITS COMPANION GALAXIES

Name	ℓ	b	s (kpc)	$v_\odot$ (km s^{-1})	r (kpc)	$v_{r\odot}$	Type
Observed Line-of-Sight Radial Velocities from Courteau & van den Bergh 1999							
M31	121.2	−21.6	770 ± 40	−301 ± 1	...	...	Sb I–II
M32	121.1	−22.0	770 ± 40	−205 ± 3	5	+95	E2
NGC 205	120.7	−21.1	830 ± 35	−244 ± 3	61	+58	dSph
NGC 147	119.8	−14.3	755 ± 35	−193 ± 3	100	+118	dSph/dE5
NGC 185	120.8	−14.5	620 ± 25	−202 ± 7	173	+107	dSph/dE3
M33	133.6	−31.5	850 ± 40	−180 ± 1	225	+72	Sc II–III
IC 10	119.0	−3.3	660 ± 65	−344 ± 5	253	−29	dIrr
LGS 3	126.8	−40.9	810 ± 60	−286 ± 4	276	−38	dIrr/dSph
Pegasus	94.8	−43.5	760 ± 100	−182 ± 2	409	+86	dIrr/dSph
IC 1613	129.7	−60.6	715 ± 35	−232 ± 5	504	−58	Irr V
Observed Line-of-Sight Radial Velocities from This Study							
And I	121.7	−24.9	790 ± 30	−380 ± 2	49	−85	dSph
And II	128.9	−29.2	680 ± 25	−188 ± 3	158	+82	dSph
And III	119.3	−26.2	760 ± 70	−355 ± 10	67	−58	dSph
And V	126.2	−15.1	810 ± 45	−403 ± 4	118	−107	dSph
And VI	106.0	−36.3	775 ± 35	−354 ± 3	265	−65	dSph
Cas dSph	128.5	−38.8	760 ± 70	−307 ± 2	244	−57	dSph

NOTE.—The heliocentric distances s are taken from Grebel (2000). Listed are Galactic coordinates (ℓ, b), the heliocentric distances s, the observed line-of-sight radial velocities $v_\odot$, the distances from the center of M31 r, corrected line-of-sight velocities $v_{r\odot}$ (adjusted for the solar motion within the Milky Way and the radial motion toward M31), and object type.

have also carried out HIRES multislit echelle observations of 21 red giant branch stars in Cas dSph. The radial velocities of the dSphs are recorded in the lower panel of Table 1.

2.2. *Distance Estimates*

In general, distance estimates for the M31 companions are derived from variable stars such as Cepheids and RR Lyrae, from the tip of the red giant branch (TRGB) method (Lee, Freedman, & Madore 1993), or from the brightness of horizontal branch (HB) stars (Lee, Demarque, & Zinn 1994). One has to rely on TRGB- or HB-based distances for the dSphs, since they lack the young stellar populations with which Cepheid variables are associated.

Deep V and B exposures with *Hubble Space Telescope*/WFPC2 have been used to clearly detect the HBs in And I and And II (Da Costa et al. 1996, 2000). The distance estimates for these galaxies are the most accurate of all the M31 dSphs. The HB method provides greater distance accuracy than the TRGB method, but HB stars are faint and difficult to photometer accurately, especially in crowded fields, and this makes the method impractical for most ground-based telescopes. Moreover, the metallicity dependence of the HB absolute magnitude M_V(HB) has been the subject of some debate (Ajhar et al. 1996). Distances based on the TRGB method are available for the rest of the M31 dSph satellites. Photometry of bright red giants has been carried out with the KPNO 4 m telescope, the 3.5 m WIYN telescope, the 6 m BTA telescope at the Special Astrophysical Observatory, and with LRIS on Keck II for the following dSphs: And III (Armandroff et al. 1993), And V (Armandroff et al. 1998; Grebel & Guhathakurta 1998), And VI (Grebel & Guhathakurta 1999; Tikhonov & Karachentsev 1999; Armandroff et al. 1999), and Cas dSph (Grebel & Guhathakurta 1999; Tikhonov & Karachentsev 1999). There are several limitations to the TRGB method: it takes a large sample size to define the TRGB break accurately; since the method involves the location of a step in the stellar luminosity function, biases in the distance estimate are caused by blends and photometric errors; errors in statistical field subtraction can be a problem; and super-TRGB populations such as intermediate-age asymptotic giant branch stars can cause systematic errors.

For all the dSphs, there is substantial error on the distances (see Table 1). Additional uncertainty is introduced through the poorly known distance of M31 itself, for which a variety of estimates is available using different methods; we adopt a distance of 770 kpc.

3. MASS ESTIMATES

Let us assume that the halo of M31 is spherically symmetric with the potential ψ and density ρ given by

$$\rho(r) = \frac{M}{4\pi}\frac{a^2}{r^2(r^2+a^2)^{3/2}},$$
$$\psi(r) = v_0^2 \log\left(\frac{\sqrt{r^2+a^2}+a}{r}\right). \quad (1)$$

The satellite galaxies are assumed to follow the same density law ρ_s but with the scale length $a_s = 250$ kpc (Evans & Wilkinson 2000). The velocity normalization v_0 is chosen to reproduce the circular speed at 30 kpc of ~235 km s^{-1} (Braun 1991). We adopt two possibilities for the distribution of velocities. These must depend on the integrals of motion, namely the binding energy ϵ and angular momentum l per unit mass. The first is a distribution function of form

$$F(\epsilon, l) = l^{-2\beta} f(\epsilon), \quad (2)$$

so that the orbital anisotropy $\beta = 1 - \langle v_\theta^2\rangle/\langle v_r^2\rangle$ is constant. This distribution ranges from radial anisotropy ($\beta > 0$) to tangential anisotropy ($\beta < 0$). The second is a distribution of Osipkov-Merritt form (see Binney & Tremaine 1987):

$$F(\epsilon, l) = f(Q), \qquad Q = \epsilon - l^2/2r_a^2, \quad (3)$$

where r_a is an anisotropy radius. This distribution is isotropic

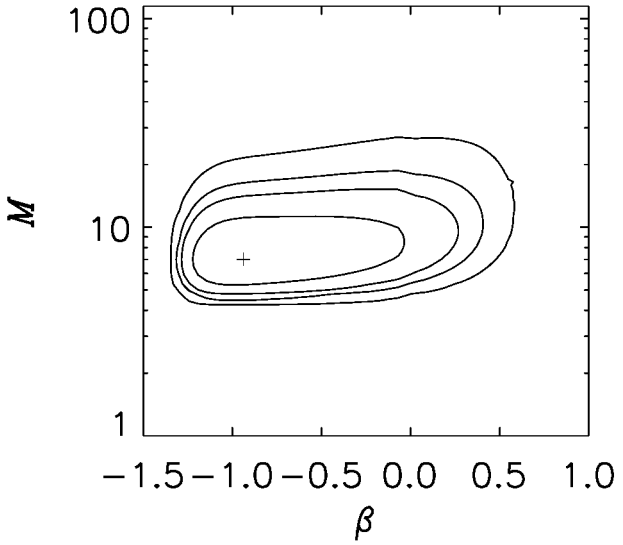

FIG. 1.—Likelihood contours in the plane of total mass M (in units of $10^{11}\ M_\odot$) and anisotropy parameter β. The contours are at heights 0.32, 0.10, 0.045, and 0.01 of the peak. The most likely mass is $7.0 \times 10^{11}\ M_\odot$, and the most likely value of β is -0.90, corresponding to tangential anisotropy.

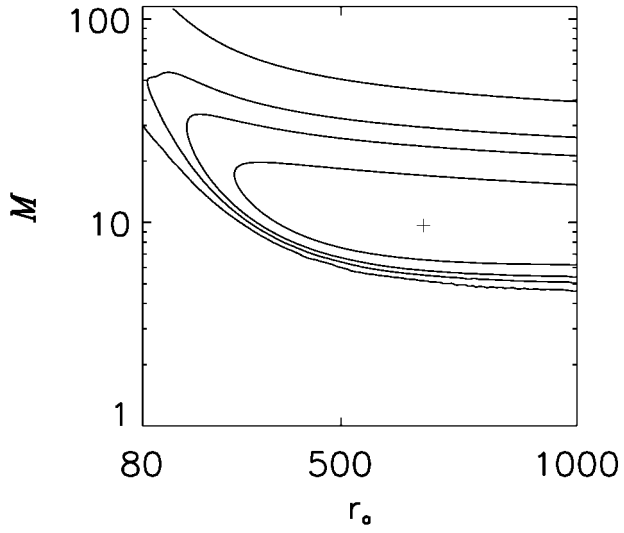

FIG. 2.—Likelihood contours in the plane of total mass M (in units of $10^{11}\ M_\odot$) and anisotropy radius r_a. The contours are at heights 0.32, 0.10, 0.045, and 0.01 of the peak. The most likely mass is $9.4 \times 10^{11}\ M_\odot$, and the most likely value of r_a is 680 kpc.

in the inner parts ($r \ll r_a$) and radially anisotropic in the outer parts ($r \gg r_a$). The functions $f(\epsilon)$ and $f(Q)$ are written out elsewhere (Wilkinson & Evans 1999; Evans & Wilkinson 2000).

Mass estimation using Bayesian likelihood methods was introduced by Little & Tremaine (1987). Bayes's theorem states that the probability of any set of model parameters given the data $P(\text{model}|\text{data})$ is

$$P(\text{model}|\text{data})P(\text{data}) = P(\text{model})P(\text{data}|\text{model}). \quad (4)$$

Here, $P(\text{model})$ describes our prior beliefs as to the likelihood of the model parameters, while $P(\text{data}|\text{model})$ is the probability of the data given the model. For the 15 satellite galaxies, the data consist of three-dimensional positions r_i with respect to the center of Andromeda, together with their heliocentric line-of-sight velocities $v_{\odot,i}$. These are corrected for the motion of the Sun around the Galactic center and the infall of the Milky Way toward Andromeda. We assume a circular speed of 220 km s^{-1} at the Galactocentric radius of the Sun ($R_\odot = 8.0$ kpc) and a solar peculiar velocity in km s^{-1} of $(U, V, W) = (-9, 12, 7)$. The line-of-sight velocity of M31, corrected for the motion of the Sun, is $v_{r,\,\mathrm{M31}} = -123$ km s^{-1} (Courteau & van den Bergh 1999). This gives the velocities $v_{r\odot,i}$ in the rest frame of the center of M31. Along any line of sight, let (v_t, η) be polar coordinates in the plane of the sky. Then the required probability is given by

$$P(\text{data}|\text{model}) = \frac{1}{\rho_s(r_i)} \int_0^{2\psi(r_i)-v_{r\odot,i}^2} dv_t\, v_t \int_0^{2\pi} d\eta\, f(\epsilon, l). \quad (5)$$

The prior probabilities contain the a priori information about the model parameters. For the total mass M, we use $P(M) \propto 1/M^2$, while for the velocity anisotropy, we use $P(\beta) \propto 1/(3-2\beta)^2$ or $P(r_a) \propto 1/r_a$ (see Wilkinson & Evans 1999 for a discussion).

The distances to the satellite galaxies are the main uncertainty. Our error convolution aims to take account of two factors. First, there is the quoted error estimate Δs_i associated with each distance given in Table 1. Second, there is a small, but distinct, probability ϵ that some of the published distance estimates are seriously in error due to systematic uncertainties; we assume that the probability of a rogue distance ϵ is 0.1. Therefore, we choose our convolution function E to have the form

$$E(z; i) = (1-\epsilon)B(z; s_i - \Delta s_i, s_i + \Delta s_i) + \epsilon B(z; s_{\min}, s_{\max}). \quad (6)$$

Here, B is the hat-box function

$$B(d; d_{\min}, d_{\max}) = \begin{cases} \dfrac{1}{d_{\max} - d_{\min}}, & d_{\min} < d < d_{\max}, \\ 0, & \text{otherwise}, \end{cases} \quad (7)$$

while s_i is the published distance estimate of the ith satellite with error Δs_i and $s_{\min}$ and $s_{\max}$ are the maximum and minimum of the distance estimates listed in Table 1.

Figure 1 shows the results for the constant anisotropy distributions. The most likely mass is $7.0 \times 10^{11}\ M_\odot$, and the most likely value of β is -0.95, corresponding to tangential anisotropy. An earlier analysis found that there is a tendency to underestimate the mass for small data sets (Evans & Wilkinson 2000). This typically leads to an underestimate of the order of a factor of 2 for a data set of 10–20 objects and is combined with a spread that is of the order of 50%. This gives a final result of $\sim 7.0^{+10.5}_{-3.5} \times 10^{11}\ M_\odot$. The anisotropy is poorly constrained as the likelihood contours are distended horizontally. However, radial anisotropy is not favored as the 1 σ contour is concentrated in the tangentially anisotropic portion of the figure. Figure 2 shows the results for the Osipkov-Merritt distribution function. The most likely mass is $\sim 9.7^{+14.6}_{-4.9} \times 10^{11}\ M_\odot$ and the most likely value of r_a is $\sim$680 kpc, suggesting that the velocity distribution is roughly isotropic. Table 2 shows the effects of varying some of our modeling assumptions on the results for the mass. These include (1) the omission of Pegasus and IC 1613, which may not be bound to M31 (Cour-

TABLE 2

ILLUSTRATION OF THE EFFECTS OF CHANGING SOME OF THE ASSUMED MODEL PARAMETERS

	Distributions of the Form $l^{-2\beta}f(\epsilon)$		$f(Q)$ Models	
Comment	Most Likely β	Most Likely M	Most Likely r_a	Most Likely M
Canonical	−0.90	7.0	680	9.4
Pegasus and IC 1613 omitted	−0.95	4.8	224	6.8
Satellite distances altered	−0.85	8.7	659	11.2
$\Delta s = 25\%$	−0.90	8.1	610	10.8
$a_s = 150$ kpc	−0.95	7.6	627	11.1
$v_c = 270$ km s^{-1}	−0.95	7.0	697	9.3
$v_c = 200$ km s^{-1}	−0.95	7.6	648	10.2

NOTE.—The parameter that has been changed is given in the first column. The second and third columns refer to distributions of the form $l^{-2\beta}f(\epsilon)$, while the fourth and fifth columns are for the $f(Q)$ models. Also recorded are the most likely values of M (in units of $10^{11}\ M_\odot$), as well as the anisotropy parameters β and r_a (in kiloparsecs).

teau & van den Bergh 1999), (2) the alteration of the satellite distances to those compiled by Mateo (1998), (3) the increase of the error bars on the distances to 25%, (4) the alteration of the scale length of the satellite galaxy number density distribution, and (5) the change of the velocity normalization of the halo v_0. The main change is the removal of Pegasus and IC 1613 from the data set, which causes a roughly 30% drop in the mass estimate. As can be seen from Table 2, the other alterations do not have a significant effect on the answer.

4. CONCLUSIONS

We have presented the first detailed study of the mass of the halo of the Andromeda galaxy that uses the radial velocity and distance measurements for all six dSph satellites (And I, And II, And III, And V, And VI, and Cas dSph). This takes to 15 the number of tracers at large radii and provides a reasonable sample with which to estimate the total mass. Such calculations have not been possible before because of the unavailability of radial velocity data for the low surface brightness companions of Andromeda. Spectroscopy of individual red giant stars in these systems has only recently become feasible thanks to 8–10 m–class telescopes such as Keck and state-of-the-art spectrographs (Côté et al. 1999; Guhathakurta et al. 2000a, 2000b). We reckon that the mass of the Andromeda halo is $\sim 7.0^{+10.5}_{-3.5} \times 10^{11}\ M_\odot$. This comes from analyzing all the companion galaxies with a family of velocity distributions of constant orbital anisotropy. The error bars include the statistical effects of the small data set, as well as the uncertainties in the distance estimators. There is some additional uncertainty from changes in the modeling assumptions, but this is at the 30% level at most. For example, altering the velocity distribution gives us a slightly higher estimate of $\sim 9.7^{+14.6}_{-4.9} \times 10^{11}\ M_\odot$.

The most recent estimate of the mass of the Milky Way is $\sim 19^{+36}_{-17} \times 10^{11}\ M_\odot$ (Wilkinson & Evans 1999). All the mass estimates inevitably come with substantial uncertainty, since they are inferred from the small data sets of satellite galaxies that are the only known probes of the distant halo. Bearing in mind such caveats, a fair conclusion is that *the Andromeda halo is very roughly as massive as that of the Milky Way*. There seems little evidence from the satellite galaxy motions for the widely held belief that the Andromeda halo is more massive than that of the Milky Way (e.g., Peebles 1996). Indeed, such evidence as there is points in the opposite direction, namely that the Andromeda halo may actually be slightly less massive.

E. K. G. acknowledges support by NASA through grant HF-01108.01-98A from the Space Telescope Science Institute, which is operated by AURA, Inc., under NASA contract NAS5-26555.

REFERENCES

Ajhar, E. A., Grillmair, C. J., Lauer, T. R., Baum, W. A., Faber, S. M., Holtzman, J. A., Lynds, C. R., & O'Neil, E. J., Jr. 1996, AJ, 111, 1110
Armandroff, T. E., Da Costa, G. S., Caldwell, N., & Seitzer, P. 1993, AJ, 106, 986
Armandroff, T. E., Davies, J. E., & Jacoby, G. H. 1998, AJ, 116, 2287
Armandroff, T. E., Jacoby, G. H., & Davies, J. E. 1999, AJ, 118, 1220
Binney, J., & Tremaine, S. 1987, Galactic Dynamics (Princeton: Princeton Univ. Press)
Braun, R. 1991, ApJ, 372, 54
Côté, P., Mateo, M., Olszewski, E. W., & Cook, K. H. 1999, ApJ, 526, 147
Courteau, S., & van den Bergh, S. 1999, AJ, 118, 337
Da Costa, G. S., Armandroff, T. E., Caldwell, N., & Seitzer, P. 1996, AJ, 112, 2576
———. 2000, AJ, 119, 705
Evans, N. W., & Wilkinson, M. I. 2000, MNRAS, 316, 929
Grebel, E. K. 1999, in IAU Symp. 192, The Stellar Content of Local Group Galaxies, ed. P. Whitelock & R. Cannon (Provo: ASP), 17
———. 2000, in 33d ESLAB Symp., Star Formation from the Small to the Large Scale, ed. F. Favata, A. A. Kaas, & C. Wilson (Noordwijk: ESA), in press (astro-ph/0005296)
Grebel, E. K., & Guhathakurta, P. 1998, BAAS, 193, 0802
———. 1999, ApJ, 511, L101
Guhathakurta, P., Grebel, E. K., Pittroff, L. C., Reitzel, D. B., Phillips, A. C., Vogt, S. S., Ostheimer, J. C., & Majewski, S. R. 2000a, AJ, submitted
Guhathakurta, P., Reitzel, D. B., & Grebel, E. K. 2000b, Proc. SPIE, 4005, 168
Karachentsev, I. D., & Karachentseva, V. E. 1999, A&A, 341, 355
Lee, M. G., Freedman, W. L., & Madore, B. F. 1993, ApJ, 417, 553
Lee, Y.-W., Demarque, P., & Zinn, R. 1994, ApJ, 423, 248
Little, B., & Tremaine, S. D. 1987, ApJ, 320, 493
Mateo, M. 1998, ARA&A, 36, 435
Oke, J. B., et al. 1995, PASP, 107, 375
Peebles, P. J. E. 1996, in Gravitational Dynamics, ed. O. Lahav, E. Terlevich, & R. J. Terlevich (Cambridge: Cambridge Univ. Press), 219
Tikhonov, N. A., & Karachentsev, I. D. 1999, Astron. Lett., 25, 332
Vogt, S. S., et al. 1994, Proc. SPIE, 2198, 362
Wilkinson, M. I., & Evans, N. W. 1999, MNRAS, 310, 645